Sound & Vibration 2024, 59(2), 1712.
https://doi.org/10.59400/sv1712

Article

Research on a broadband vibration energy acquisition method combining nonlinear softening and hardening

Peng Wang[1,2,*], Xiaoyan Fu[2], Chen Li[2], Renwen Chen[1,*]

[1] State Key Laboratory of Mechanics and Control for Aerospace Structures, Nanjing University of Aeronautics and Astronautics, Nanjing 210016, China
[2] Xinjiang Railway Vocational and Technical College, Urumqi 830011, China
* Corresponding author: Peng Wang, 6734078@qq.com; Renwen Chen, rwchen@nuaa.edu.cn

Wang P, Fu X, Li C, Chen R. Research on a broadband vibration energy acquisition method combining nonlinear softening and hardening. Sound & Vibration. 2024; 59(2): 1712. https://doi.org/10.59400/sv1712

ARTICLE INFO

Received: 9 September 2024
Accepted: 6 November 2024
Available online: 21 May 2025

Abstract: The main content of this article is to study and analyze the nonlinear dynamic behavior of a flexible buckling vibration piezoelectric energy harvesting device, and design a wideband piezoelectric energy conversion device using a double-layer stacked buckling configuration. During the research process, the technical situation of regulating nonlinear softening/hardening vibration response was deeply explored, and a systematic analysis was conducted on the optimization strategy of broadband vibration energy harvesting under the coupling of soft and hard nonlinear effects. This study provides a theoretical basis for subsequent scholars to expand academic research in related fields.

Keywords: energy harvesting technology; piezoelectric materials; nonlinear dynamics; structural optimization; vibration control; energy conversion efficiency, renewable energy systems; self-powered sensors

1. Introduction

The energy supply demand of large-scale wireless sensor network nodes in intelligent connected systems and the limited wired power supply in certain special environments have made batteries the main energy supply method currently [1]. Therefore, due to the limited lifespan of batteries, it also leads to difficulties in maintenance, increases the degree of environmental pollution, and easily triggers various potential safety risks. This series of situations has promoted the development of related technologies for mobile phone energy, hoping that it can replace batteries and solve these problems caused by battery power supply. Among them, piezoelectric energy harvesting technology has been widely studied due to its advantages of simple structure and high-power density [2]. However, traditional silicon-based piezoelectric energy harvesters are limited by stiffness, making it difficult to achieve efficient energy conversion of a large number of low-frequency vibration sources in the environment [3]. In addition, with the rapid development of flexible electronic technology in wearable electronics, implantable medical electronics, and other fields, there is an urgent need for compatible and integrated flexible energy harvesting technologies to overcome the limitations of batteries on their flexible development [4]. With the continuous increase of low-power products, the efficient utilization of energy has also attracted widespread attention, among which the stability of environmental energy has received the attention of many scholars. How to improve stability has become the focus of current research [5]. Therefore, This study constructs a flexible buckling piezoelectric energy capture and conversion theoretical framework applicable to forced vibration conditions, systematically investigates the energy conversion dynamic mechanism of the structure under low-frequency forced vibration excitation, and focuses on revealing the high-frequency displacement behavior characteristics caused by nonlinear stiffness enhancement effect and the low-frequency displacement response law caused by nonlinear stiffness weakening effect. By exploring the technical path and optimization strategy for stable wideband vibration energy harvesting, the practical value of nonlinear vibration energy harvesting devices in engineering applications has been effectively enhanced. Ultimately, an innovative manufacturing process for high-power density low-frequency wideband piezoelectric energy harvesters with high spectral utilization has been developed.

2. Flexible buckling nonlinear broadband piezoelectric vibration energy harvesting method and related experiments

2.1. Structural design and preparation

Figure 1a shows a 3D schematic of a flexible buckling bridge piezoelectric energy harvester (PEH) manufactured using thin PZT thick film. The device structure consists of three key components: piezoelectric ceramic element, metal substrate, and polymer support layer. Firstly, piezoelectric thin film single crystal elements were prepared from metal substrates using hot pressing bonding and mechanical thinning processes. Piezoelectric ceramic blocks with bottom electrodes Cr/Au (20 nm/200 nm) sputtered (thickness 300 μm and length 16 mm PZT, C-6, Fuji ceramics, Japan) were bonded to beryllium bronze layers (thickness 50 μ m and length 20 mm) for 3.5 h under a bonding pressure of 0.2 MPa in a vacuum oven at 175 ℃. Then, piezoelectric is thinned to 50 μm through mechanical thinning process, and Cr/Au (20 nm/200 nm) was sputtered on surface of the piezoelectric layer using polyimide tape as a hard mask. Due to the different thermal expansion coefficients between the piezoelectric layer and the beryllium bronze substrate material, the high temperature treatment through bonding and the low stiffness characteristics after thinning result in a certain initial bending curvature (bending angle less than 2°) of the single crystal wafer. Finally, maintaining the same width, the piezoelectric single crystal is bonded together with a 100 μm thick polyethylene terephthalate (PET) sheet using epoxy resin adhesive. The composite layer structure is fixed at the end with a distance of 25 mm between the two ends in a natural state, The symmetrical effect of the structure is shown in **Figure 1b**. The PET layer serves as a flexible substrate for the piezoelectric single crystal sheet, lowering the bending stiffness during vibrational deformation and enabling operation at low frequencies. To enhance buckling deformation and improve piezoelectric energy conversion efficiency, a T-shaped tungsten mass block is integrated at the center of the buckling bridge structure (dimensions: top—10 × 1 × 5 mm^3, bottom—2 × 1.5 × 5 mm^3). This design also helps reduce the system's resonant frequency, as illustrated in **Figure 1c**. In addition, the bending characteristics of the bonded piezoelectric single crystal wafer shown in **Figure 1d** indicate that the structure has good flexibility.

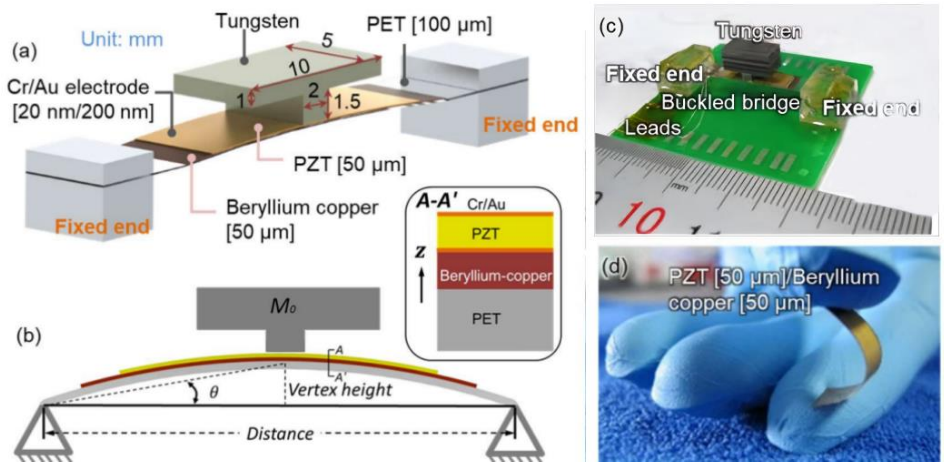

Figure 1. Collector structure. (**a**) 3D model description; (**b**) Equipment cross-sectional plane; (**c**) Equipment photos; (**d**) Flexibility assessment.

2.2. Open circuit output characteristics

Figure 2a shows the output voltage with acceleration amplitudes ranging from 0.01 g to 2.0 g at frequencies of 70 Hz to 110 Hz. Experimental results indicate that the peak output voltage ranges between 0.17 V and 15.18 V during the positive scan, while dropping to 11.64 V in the negative scan. Under high-acceleration excitation, the plateau characteristic of the output voltage curve becomes more pronounced, with the peak voltage shifting toward the higher frequency region—a clear manifestation of hardening nonlinearity [4,5].

Specifically, when the frequency gradually increases along the forward direction from 70 Hz, the piezoelectric buckling bridge vibration energy harvester first vibrates around its initial position with small deformations, and the output voltage continuously increases; Next, the first forward jump of the output is generated by buckling the piezoelectric bridge at 78.5 Hz; As the frequency continues to increase, at 93.4 Hz, the buckling bridge begins to enter an unstable output state region (i.e., the high-energy output between the hysteresis curves). At 105.3 Hz, a sudden drop in voltage is observed, and the vibration amplitude of the piezoelectric bridge also suddenly decreases, indicating that it maintains small deformation oscillations around its stable initial position again [6].

The frequency of voltage occurrence (**Figure 2b**) and the maximum output peak voltage value (**Figure 2c**) show the same conclusion as the amplitude of excitation acceleration increases. In the range of relatively small acceleration, as the value increases, the response frequency of the maximum peak voltage gradually decreases. This is mainly attributed to the increased elastic flexibility of PZT under high stress and the softening nonlinear effect of piezoelectric materials [7]. When the applied external acceleration amplitude exceeds the critical threshold of 0.25 g, the system response frequency shows a trend of shifting towards the high frequency band, which is mainly attributed to the stiffness enhanced nonlinear characteristics unique to buckling structures. When the amplitude of the excitation acceleration further increases to over 0.7 g, the frequency response curves obtained through bidirectional scanning tests exhibit more significant phase lag intervals, indicating that the system exhibits more complex nonlinear dynamic behavior under strong excitation conditions. As shown in **Figure 2c**, under low excitation conditions, similar to a general piezoelectric vibration energy harvester [8–10], the output peak voltage has a linear relationship with the applied acceleration amplitude, and nonlinear phenomena occur at acceleration amplitudes exceeding 0.25 g. In addition, bandwidth is defined as the frequency band between two frequencies when the output voltage amplitude is −3 dB of the peak. Therefore, when the acceleration is 0.5, 0.7, 1.0, and 2.0 g, the bandwidth of the frequency domain curve obtained from the forward sweep test gradually increases from 5 Hz, 7 Hz, 10 Hz to 15 Hz, respectively.

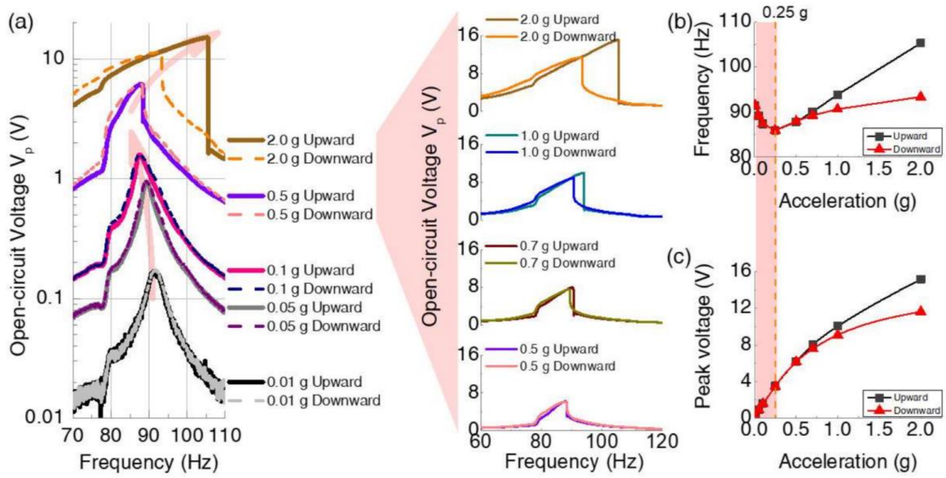

Figure 2. Collector bending bridge output. (**a**) Frequency dependence of output voltage at different amplitudes ranging from 0.01 to 2.0 g. Enlarged image: frequency scanning details; (**b**) Resonance frequency of peak voltage; (**c**) The relationship between voltage and acceleration amplitude.

Figure 3a presents both the voltage output profile and phase response of the buckling bridge piezoelectric energy harvester when subjected to 2.0 g excitation amplitude. It can be seen that there is also a 180° sudden change in phase angle at the voltage generation jump point. For the positive sweep frequency measurement, the phase angle curve jumps from ± 180° to 0°/360°, and for the negative sweep frequency measurement, the phase angle curve jumps from 0°/36 ° to ± 180°. This phenomenon can also be seen from the output waveform. **Figure 3b** shows the excitation acceleration waveforms at frequencies of 70, 85, 100, and 110 Hz, as well as the corresponding output voltage waveforms of the energy harvester. Here, the vibration excitation acceleration and frequency of the exciter are set before the experiment starts, and remain unchanged throughout the experiment. It can be seen that under the same excitation conditions, the phase difference between the jump point before and after is exactly 180°. At the same time, it can also be seen that when the fixed frequency is in the hysteresis range, the output voltage is chosen to be low-energy output, which is consistent with the typical conclusion described by nonlinear vibration theory that high-energy orbits are unstable compared to low-energy orbits.

2.3. Closed circuit output characteristics

Under constant excitation parameters, power characteristics of the piezoelectric vibration energy harvesting system are significantly correlated with the external load resistance. When the load resistance is adjusted to the optimal matching state, the system output power reaches its peak level. This characteristic indicates that energy conversion efficiency can be maximized through impedance matching optimization, providing a theoretical basis for the engineering application of piezoelectric energy harvesting devices. **Figure 4a** shows the positive and negative sweep frequency curves of the closed-loop output voltage when the external load resistance is between 5 kΩ and 200 kΩ under the acceleration amplitude of 2.0 g excitation. According to the $P_{average} = \frac{V_p^2}{2\,\mathrm{Re}\,sis\,\tan ce}$ formula, the relationship curve between the effective output power of the high-energy orbit and the load resistance is calculated as shown in **Figure 4b**. The optimal matching resistance should be around 100 kΩ, and the maximum effective output power that can be achieved is 0.6 mW. **Figure 4c** shows the impedance analysis results obtained through impedance analyzer testing. The resonance frequency and anti-resonance frequency are 86.6 Hz and 92.9 Hz, respectively. The optimal matching impedance at the resonance frequency is 120 kΩ, which is in good agreement with the closed-loop analysis results. The phase angle peak appears at 90.2 Hz, and the frequency domain curve of the open circuit under low acceleration excitation shows that this frequency highly matches the resonance frequency of the system, verifying the effectiveness of the open circuit and closed-circuit test results.

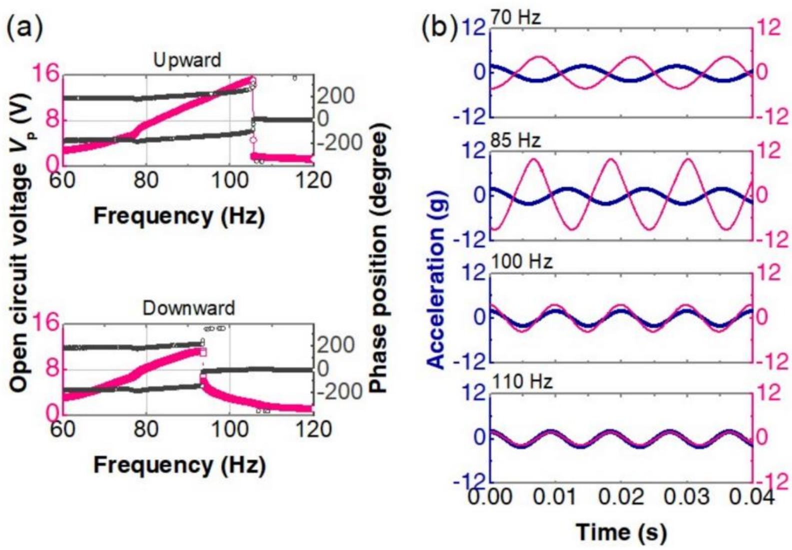

Figure 3. Folding bridge PEH voltage waveform phase. (**a**) Under an acceleration amplitude of 2.0 g; (**b**) Voltage waveforms and corresponding excitation accelerations at frequencies of 70, 85, 100, and 110 Hz.

2.4. Stability

In order to verify the reliability of the buckling bridge type piezoelectric energy harvester and the stability of the piezoelectric energy conversion output, the thickness of the top mass block structure was increased to 4 mm to achieve a concentrated load on the large mass block. The buckling bridge type vibration energy harvester was subjected to frequency domain testing at a high acceleration of 2.0 g. After 30 consecutive cycles, it was found that its hysteresis characteristics were more obvious, forming a broadband output of 30 Hz (67 Hz to 97 Hz) (as shown in **Figure 5**), and the output repeatability was good. In addition, the output performance of the buckling bridge type nonlinear vibration energy harvester was compared with similar studies in recent years, and the results are shown in **Table 1**. Among them, the construction differences and complexity of the buckling type vibration energy harvester are relatively large, and the density of the mass blocks used is not uniform. In addition, the non-linear vibration energy harvester mainly considers the output characteristics, so the volume in the formula only calculates the effective volume of the functional piezoelectric material. In summary, compared to the studies reported in recent years, the bending bridge vibration energy harvester based on PET supported metal substrate piezoelectric thin film has higher output power and normalized power density.

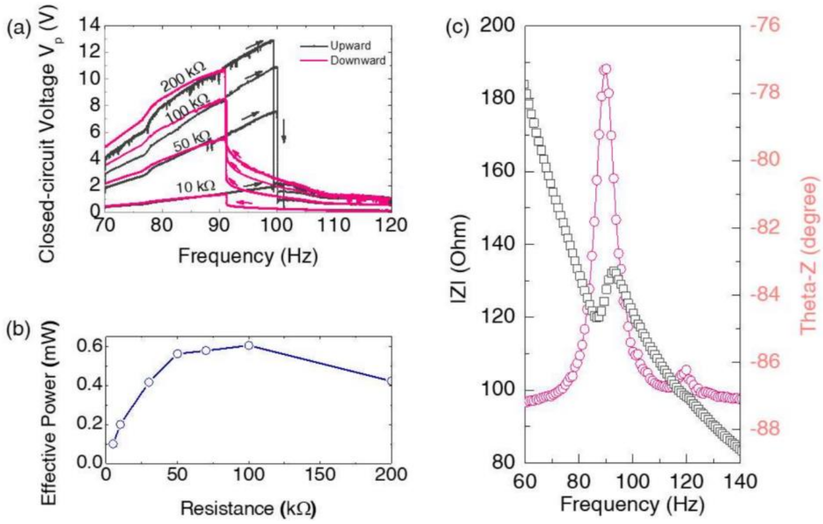

Figure 4. Power and impedance. (**a**) Closed circuit voltage scanned up and down frequency under different resistances; (**b**) The relationship between power and load under 2.0 g acceleration; (**c**) Impedance spectrum of equipment

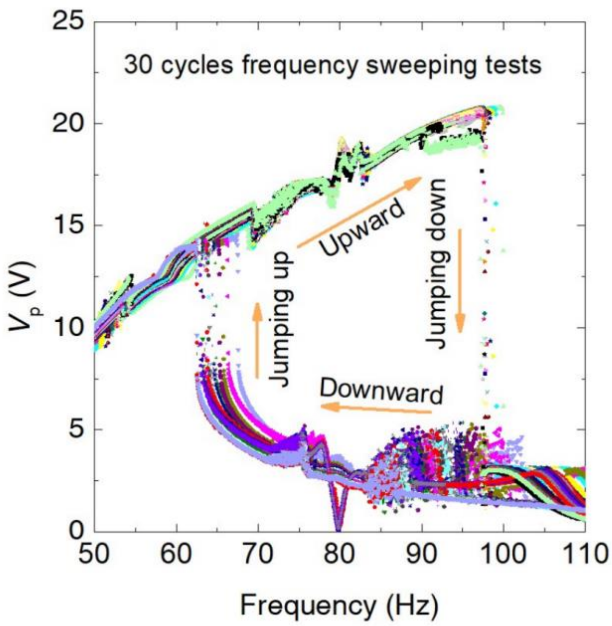

Figure 5. The stability evaluation.

Table 1. Comparison of Bridge PEHs.

Material	piezoelectric layer volume	acceleration	bandwidth	frequency	power	power density	normalized power density	reference
PVDF	1.664	3	22	30	29	1.74	0.0064	Jung [11]
MFC	457.2	0.5	4.5	68	100	0.22	0.0129	Gafforelli [12]
PVDF	131.2	14	-	-	61.8	0.47	-	Zhang [13]
PZP	60	-	-	3	5	0.083	-	Jiang [14]
PZP	42.24	-	-	14	48	1.36	-	Xie [15]
PZP	4	2	15	105.3	600	150	0.3561	Ours

In summary, a preparation scheme for a flexible polymer supported piezoelectric buckling bridge type nonlinear vibration energy harvester using a metal substrate piezoelectric thin film preparation process was proposed. Combined with the design of a *T*-shaped mass block, the thermal stress naturally buckling piezoelectric bridge generated nonlinear vibration energy conversion under a low excitation acceleration of about 0.25 g. When the applied acceleration amplitude was 2.0 g, a bandwidth of about 15 Hz could be maintained. The device demonstrates excellent energy conversion performance, delivering 0.6 mW of peak power with a corresponding volumetric power density of 150 mW/cm^3 when subjected to 2.0 g acceleration at 105.3 Hz excitation. Furthermore, its performance metrics include a remarkable normalized power density of 0.36 $mW\cdot cm^{-3}\cdot g^{-2}\cdot Hz^{-1}$, while the thin-film buckling bridge architecture exhibits outstanding operational stability.

3. Broadband energy harvesting method and corresponding experiments combining nonlinear softening and hardening effects

As a representative nonlinear configuration, buckling bridges enable broadband piezoelectric energy harvesting [6]. These systems exhibit bistable behavior in their frequency hysteresis zone, featuring both high-energy (unstable) and low-energy (stable) operational modes [14,16–20]. For practical implementation with vibration sources of fixed frequency ranges, obtaining consistent high-energy output is particularly valuable. Consequently, enhancing broadband stability in nonlinear energy harvesters has emerged as a key research focus [11,21–25]. To address this challenge, we introduce an innovative approach that synergistically combines hardening and softening nonlinearities in vibration energy harvesters. The methodology involves:

Fabricating two distinct buckling-drum piezoelectric harvesters with controlled nonlinear properties through precise buckling angle adjustment

Engineering the low-frequency resonator to exhibit hardening behavior while the high-frequency device demonstrates softening characteristics

When properly tuned to overlap at specific acceleration levels, this dual-resonator system eliminates energy output discontinuities, enabling seamless ultra-wideband performance. The proposed configuration significantly improves the practical utility of nonlinear energy harvesting systems.

Figure 6a illustrates the three-dimensional configuration of the drum-type piezoelectric energy harvester, featuring a compliant eardrum structure fabricated from PET substrate, stainless steel foil, and PZT thin film. Firstly, the raw material blocks of different layers are patterned by UV laser method. Then, the composite layer structure composed of stainless steel and PZT is prepared by the piezoelectric film composite structure preparation process of metal substrate. Finally, the piezoelectric chip is bonded to the patterned PET substrate by epoxy resin adhesive to manufacture the piezoelectric buckling eardrum structure. The four supporting edges of the bending drum are fixed on a rigid base of 3D printing, and the mushroom shaped mass block is assembled at the center of the drum to provide concentrated force. During the fixation process, different bending angles are prepared by controlling the preset heights of different center points, with bending 2° and 5° respectively, as shown in **Figure 6b**.

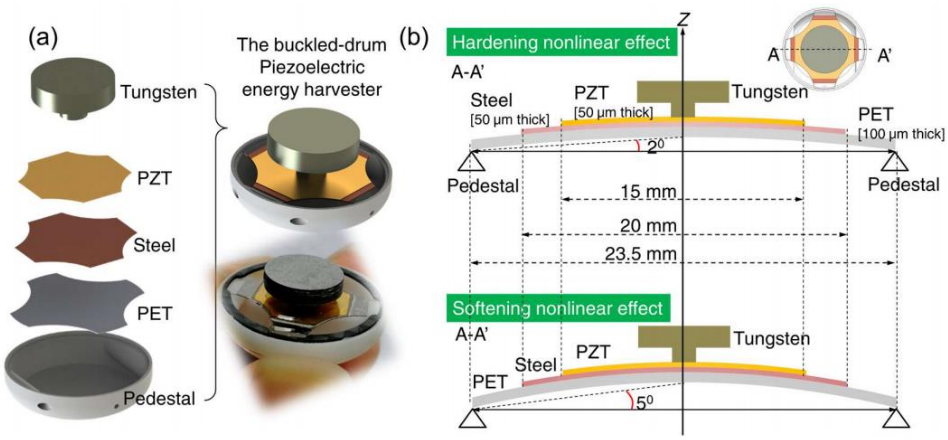

Figure 6. Figure 1 presents the structural configuration of the buckled-drum piezoelectric energy harvester. (**a**) Conceptual diagram and physical prototype of the device; (**b**) Operational principles showing both hardening nonlinear behavior (2° buckling angle) and softening nonlinear characteristics (5° buckling angle).

Figure 7 The open-circuit voltage response was measured across a frequency spectrum of 60–160 Hz under varying acceleration levels (0.1, 0.5, and 1.0 g). Results demonstrate that the two PEHs produce contrasting nonlinear voltage outputs. With increasing excitation amplitude, the operational bandwidth expands considerably, while the hysteresis between forward and reverse frequency sweeps becomes more pronounced. As shown in **Figure 7a**,**b**, the frequency domain analysis under a low acceleration amplitude of 0.1 g shows that the first-order resonance frequencies of the two are 93 Hz and 134 Hz, respectively.

At elevated excitation levels, the system demonstrates distinct nonlinear behaviors depending on buckling angle: a 2° angle induces hardening nonlinearity, shifting voltage output toward higher frequencies, whereas a 5° angle produces softening nonlinearity, causing frequency response to migrate toward lower bands. As shown in the figure, under the excitation condition of a 2.0 g acceleration amplitude, the stable bandwidth with a peak voltage greater than 4 V at a buckling angle of 2 is about 40 Hz and the unstable bandwidth is about 17 Hz. For a buckling angle of 5, the stable bandwidth with a peak voltage greater than 4 V is about 37 Hz and the unstable bandwidth is about 15 Hz. Furthermore, the frequency shift observed at 5° buckling angle is significantly greater than at 2°, primarily due to the reversal of nonlinear effects that occurs under high excitation accelerations with larger buckling angles.

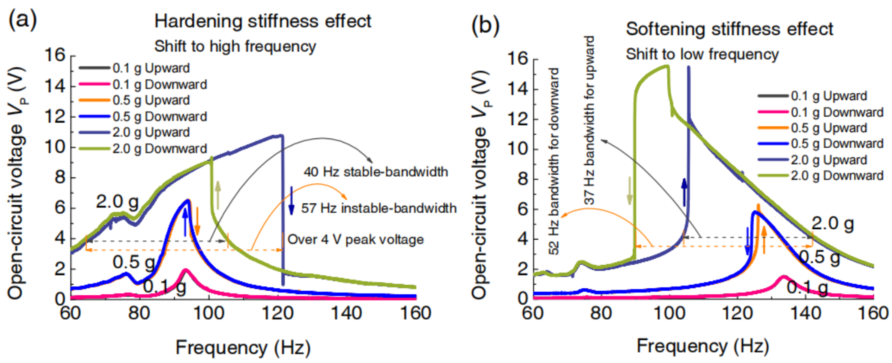

Figure 7. Structural design of energy harvester. **(a)** Schematic diagram; **(b)** Schematic diagram of the crushing drum collector with a hardening nonlinear mechanism (crushing angle of 2 °) and a softening nonlinear mechanism (crushing angle of 5 °).

In order to avoid the jumping phenomenon of low energy output, the study will output two vibration energy harvesters with different nonlinear effects in parallel and series. Due to the opposite direction of frequency shift, when the external excitation acceleration amplitude reaches an appropriate value, the frequency domain curve will meet at a specific frequency, and the jumping phenomenon of low energy output will be eliminated. **Figure 8** shows the parallel and series open circuit outputs of the two under different excitation acceleration amplitudes of 1.0 g, 1.5 g, and 2.0 g. It can be observed that the hysteresis characteristics of the positive and negative frequency domain curves can still be observed. At an acceleration of 1.0 g, there are two low energy wells located in different frequency regions, caused by the jumps in the low energy outputs of the two energy harvesters. However, it is worth noting that the low energy trap disappears in the output curves of 1.5 g and 2.0 g, and the included jump points are all towards high energy, achieving broadband high energy output. As shown in the Figure, under the excitation acceleration amplitude of 2.0 g, the bandwidth of the peak voltage greater than 4 V reaches parallel 45 Hz and series 93 Hz, respectively.

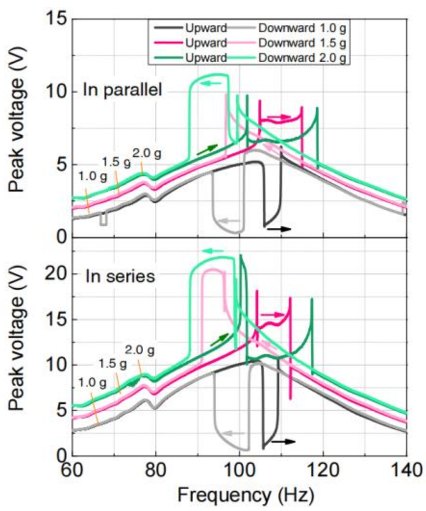

Figure 8. measures the circuit voltage response of both parallel- and series-connected PEHs under varying acceleration levels (1.0 g, 1.5 g, and 2.0 g), comparing their respective energy harvesting mechanisms.

Figure 9 shows the comparison of closed-loop output performance when the acceleration amplitude is 1.0 g, with matching resistors all at 20 kΩ. When the bending angle is 2°, the maximum output power reaches 0.7 mW (forward sweep) and 0.4 mW (negative sweep), and the maximum output current is 0.37 mA (forward sweep) and 0.26 mA (negative sweep). As for the maximum output power and current at a bending angle of 5, the maximum values reached during forward and negative sweeping are the same, with a maximum output power of 0.6 mW and a maximum output current of 0.35 mA.

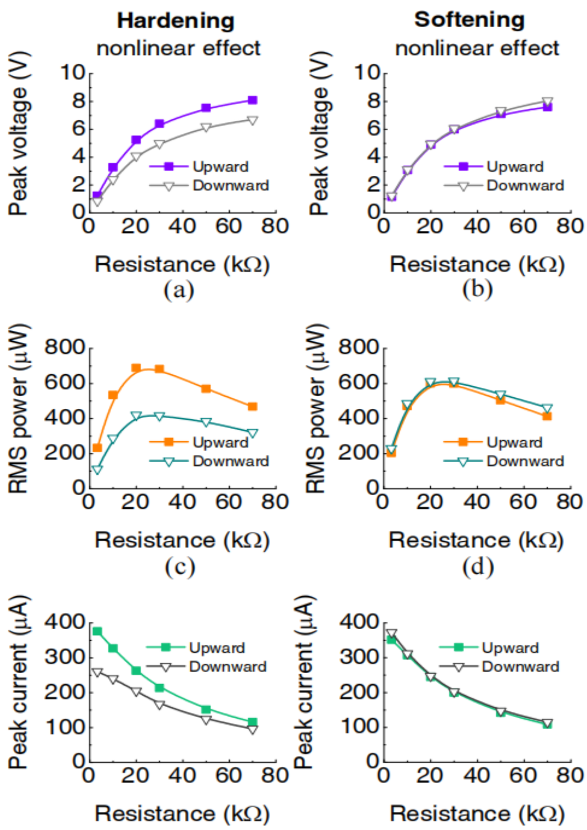

(e) **(f)**

Figure 9. The closed-circuit power generation characteristics of buckled piezoelectric energy harvesters (PEHs) were evaluated under hardening and softening nonlinear responses at an acceleration level of 1.0 g. (**a**) Output voltage of the hardening PEH (2° buckling angle); (**b**) Output voltage of the softening PEH (5° buckling angle); (**c**) Output power of the hardening PEH; (**d**) Output power of the softening PEH; (**e**) Output current of the hardening PEH (20 kΩ load); (**f**) Output current of the softening PEH (20 kΩ load).

In summary, a nonlinear vibration energy harvester with softening and hardening nonlinear effects has been manufactured, with a reasonable controller resonance frequency. By combining the high-frequency offset characteristics of the nonlinear hardening effect and the low-frequency offset characteristics of the nonlinear softening effect, combined with their advantages, it is expected to achieve a stable ultra-wideband vibration energy conversion effect and improve the practical application value of the nonlinear vibration energy harvester.

4. Conclusion

This paper presents the development of a flexible piezoelectric energy harvester with buckling capabilities, fabricated through a mechanical thinning process for piezoelectric thin films. The study investigates its broadband performance characteristics. Theoretical analysis reveals the energy conversion mechanism of the buckling piezoelectric bridge structure under nonlinear vibrations. By leveraging the high-frequency shift induced by nonlinear hardening and the low-frequency shift from nonlinear softening, stable broadband energy harvesting is realized. Experimental validation confirms the feasibility of this approach, highlighting its theoretical significance for advancing the practical use of nonlinear vibration-based energy harvesters.

Author contributions: Conceptualization, PW and RC; methodology, RC; software, XF and CL; validation, PW, XF and CL; formal analysis, PW; investigation, XF; resources, RC; data curation, XF and CL; writing—original draft preparation, PW; writing—review and editing, PW and RC; visualization, CL; supervision, RC; project administration, PW; funding acquisition, RC. All authors have read and agreed to the published version of the manuscript.

Institutional review board statement: Not applicable.

Informed consent statement: Not applicable.

Conflict of interest: The authors declare no conflict of interest.

References

1. Adeodato A, Vignoli LL, Savi AM, et al. Adaptive piezoelectric energy harvester using a shape memory alloy stopper. Nonlinear Dynamics. 2025; 1–22.
2. Li Y, Yang X, Yuan C, et al. Optimized output of piezoelectric energy harvesters with coaxial PVDF/PAN/CNT composite fibers. Sensors and Actuators: A. Physical. 2025; 388: 116450.
3. Chen Y, Zhang H, Wang G, et al. A novel magnet-spring synergistic orthogonal piezoelectric vibration energy harvester. Mechanical Systems and Signal Processing. 2025; 230: 112600.
4. Hou C, Du X, Dang S, et al. A broadband and multiband magnetism-plucked rotary piezoelectric energy harvester. Energy. 2024: 302: 131846.
5. Cai Z, Zhou K, Yang T, et al. Analysis of Dynamic Characteristics of Tristable Exponential Section of Piezoelectric Energy Harvester. Energies. 2023: 16(18): 6609.
6. Elgamal MA, Elgamal H, Kouritem SA. Optimized multi-frequency nonlinear broadband piezoelectric energy harvester designs. Scientific Reports. 2024; 14(1): 11401.
7. Hyo-Kyung S, Shuailing S, Hyun-Soo K, et al. On a nonlinear broadband piezoelectric energy harvester with a coupled beam array. Applied Energy. 2022; 328: 120129.
8. Adeodato A, Vignoli LL, Savi AM, et al. Adaptive piezoelectric energy harvester using a shape memory alloy stopper. Nonlinear Dynamics. 2025; 1–22.
9. Ren Z, Deng S, Shao J, et al. Ultrahigh-power-density flexible piezoelectric energy harvester based on freestanding ferroelectric oxide thin films. Nature Communications. 2025; 16(1): 3192–3192.
10. Ashutosh A. A review on the performance enhancement techniques of piezoelectric energy harvesters. Nanomaterials and Energy. 2025; 1–22.
11. Jung S-M, Yun K-S. Energy-harvesting device with mechanical frequency-up conversion mechanism for increased power efficiency and wideband operation. Applied Physics Letters. 2010; 96: 111906.

12. Gafforelli G, Corigliano A, Xu R, Kim S-G. Experimental verification of a bridgeshaped, nonlinear vibration energy harvester. Applied Physics Letters. 2014; 105: 203901.
13. Zhang J, Zhang J, Shu C, Fang Z. Enhanced piezoelectric wind energy harvesting based on a buckled beam. Applied Physics Letters. 2017; 110: 183903.
14. Jiang X-Y, Zou H-X, Zhang W-M. Design and analysis of a multi-step piezoelectric energy harvester using buckled beam driven by magnetic excitation. Energy Conversion and Management. 2017; 145: 129–137.
15. Xie Z, Kitio Kwuimy CA, Wang Z, et al. A piezoelectric energy harvester for broadband rotational excitation using buckled beam. Aip Advances. 2018; 8(1): 015125.
16. Lucente D, Manacorda A, Plati A, et al. Optimal Control of an Electromechanical Energy Harvester. Entropy. 2025; 27(3): 268–268.
17. Zhang X, Shan X, Sui G, et al. Enhancing piezoelectric energy harvesters with rotating triangular auxetic structures. International Journal of Mechanical Sciences. 2025; 289: 110081.
18. Cottone F, Vocca H, Gammaitoni L. Nonlinear energy harvesting. Physical Review Letters. 2009; 102: 080601.
19. Yi Z, Hu Y, Ji B, Liu J, Yang B. Broad bandwidth piezoelectric energy harvester by a flexible buckled bridge. Applied Physics Letters. 2018; 113: 183901.
20. Arrieta AF, Delpero T, Bergamini AE, Ermanni P. Broadband vibration energy harvesting based on cantilevered piezoelectric bi-stable composites. Applied Physics Letters. 2013; 102: 173904.
21. Ray RA, Koley S. Performance of piezoelectric beam type energy harvester under flow-induced vibration. Scientific Reports. 2025,15(1): 13433–13433.
22. Ebrahimi F, Parsi M. Utilizing star-shaped auxetic metabeams for piezoelectric vibration energy harvesting. Acta Mechanica. 2025; 1–25.
23. Touairi S, Ghalim N, Ouaomar H, et al. Optimization strategies for cost-effectiveness in piezoelectric energy harvesting systems. International Journal of Dynamics and Control. 2025; 13(4): 156–156.
24. Lei Q, Mu K, Wu W, et al. Analytical investigation and optimization of a vortex-induced piezoelectric energy harvester by differential transform method and response surface methodology. Archive of Applied Mechanics. 2025; 95(4): 96.
25. Thomas SE, Rajan R. Improved piezoelectric energy harvester design using aluminum nitride for improved voltage and power output. Applied Nanoscience. 2025; 15(2): 10.